Available online at www.sciencedirect.com

ScienceDirect

Geochimica et Cosmochimica Acta 123 (2013) 358–367

Geochimica et Cosmochimica Acta

www.elsevier.com/locate/gca

Short lived ^{36}Cl and its decay products ^{36}Ar and ^{36}S in the early solar system ☆

G. Turner [a,*], S.A. Crowther [a], R. Burgess [a], J.D. Gilmour [a], S.P. Kelley [b], G.J. Wasserburg [c]

[a] School of Earth, Atmospheric and Environmental Sciences, University of Manchester, Manchester M13 9PL, UK
[b] Planetary and Space Sciences Research Institute, Open University, Milton Keynes MK7 6AA, Bucks, UK
[c] Lunatic Asylum, Division of Earth and Planetary Science, California Institute of Technology, Pasadena, CA, USA

Received 10 December 2012; accepted in revised form 21 June 2013; available online 2 July 2013

Abstract

Variable excesses of ^{36}S have previously been reported in sodalite in the Allende and Ningqiang meteorites and used to infer the presence of ^{36}Cl in the early solar system. Until now no unambiguous evidence of the major decay product, ^{36}Ar (98%), has been found. Using low fluence fast neutron activation we have measured small amounts of ^{36}Ar in the Allende sodalite Pink Angel, corresponding to $^{36}Cl/^{35}Cl = (1.9 \pm 0.5) \times 10^{-8}$. This is a factor of 200 lower than the highest value inferred from ^{36}S excesses in sodalite. High resolution I–Xe analyses confirm that the sodalite formed between 4561 and 4558 Ma ago. The core of Pink Angel sodalite yielded a precise formation age of 4559.4 ± 0.6 Ma. Deposition of sodalite containing live ^{36}Cl, seven million years or so after the formation of the CAI, appears to require a local production mechanism involving intense neutron irradiation within the solar nebula. The constraint imposed by the near absence of neutron induced ^{128}Xe is most easily satisfied if the ^{36}Cl were produced in a fluid precursor of the sodalite. The low level of ^{36}Ar could be accounted for as a result of residual *in-situ* ^{36}Cl decay, up to 1–2 Ma after formation of the sodalite, and/or later diffusive loss, in line with the low activation energy for Ar diffusion in sodalite.

1. INTRODUCTION

In this study we establish, from a detailed analysis of Ar isotopes in the Allende sodalite, Pink Angel, the presence of ^{36}Ar from the in-situ decay of ^{36}Cl produced by neutron capture on ^{35}Cl in the early solar system. The $^{36}Cl/^{35}Cl$ ratio inferred, $\sim 2 \times 10^{-8}$, is a factor of 200 lower than that inferred from ^{36}S (Hsu et al., 2006) and it follows that if ^{36}Cl were present at this high level substantial loss of ^{36}Ar must have occurred at some time. Following on the early study by Swindle et al. (1988), we have carried out a more detailed investigation of the I–Xe chronology and diffusion characteristics of Xe and Ar of Pink Angel in order to present a careful comparison with the ^{36}Ar problem.

The isotope ^{36}Cl ($t_{½} = 3 \times 10^5$a) decays to ^{36}Ar (98%) and ^{36}S (2%). The dominant effects from the presence of this nuclide should appear in excesses of ^{36}Ar correlated with Cl. Such effects have never been found in Cl rich materials such as the Pink Angel, a sample which clearly contains ^{129}Xe (Villa et al., 1981) from the decay of ^{129}I ($t_{½} = 1.57 \times 10^7$a). However recent workers have shown excesses of ^{36}S, in some cases well correlated with $^{35}Cl/^{34}S$, in sodalite ($Na_8Al_6Si_6O_{24}Cl_2$) and wadalite ($Ca_6Al_5Si_2O_{16}Cl_3$) in CAIs and chondrules from the Allende and Ningqiang meteorites. These workers infer these effects as due to the presence of ^{36}Cl in the early solar system (Lin et al., 2005; Hsu et al., 2006; Ushikubo et al., 2007; Jacobsen et al.,

* Corresponding author. Tel.: +44 161 2750401.
E-mail address: grenville.turner@manchester.ac.uk (G. Turner).

0016-7037/$ - see front matter © 2013 The Authors. Published by Elsevier Ltd. All rights reserved.
http://dx.doi.org/10.1016/j.gca.2013.06.022

2009, 2011; Wasserburg et al., 2011). In general, the implied $^{36}Cl/^{35}Cl$ ratios are variable ranging from essentially zero to 4×10^{-6} for the Allende sodalite rich inclusion, Pink Angel, and to $^{36}Cl/^{35}Cl \geqslant 1.8 \times 10^{-5}$ for wadalite in the Allende type B inclusion, AJEF. In spite of the fact that ^{36}Cl decays predominantly to ^{36}Ar, all attempts to locate the very large amounts of ^{36}Ar implied by these ^{36}S excesses have been negative. Bulk ^{36}Ar concentrations in Pink Angel, combined with a typical Cl concentration of around 7%, correspond to $^{36}Ar/^{35}Cl \leqslant 10^{-8}$ (Villa et al., 1981), which is 2 orders of magnitude lower than the value implied by some of the sulphur isotope measurements.

If the inferred high ^{36}Cl abundances were the result of pre-solar nucleosynthesis, this would require a very short time scale ($\ll 10^6$a) for incorporation into the solar system. Further, it has become evident that no known stellar source is capable of producing large inventories of ^{36}Cl and it has been suggested that energetic charged particle irradiation (SEP) of solids by the early sun could be the source. This would imply coproduction of other short lived isotopes including ^{26}Al. The observed levels of ^{26}Al are too low compared to the ^{36}Cl levels in the same samples inferred above for a solid target. This would appear to eliminate the SEP source, unless the target were water /ice very depleted in refractory elements in which case ^{26}Al and neutron capture on nuclides such as ^{149}Sm and ^{157}Gd would not be present (Jacobsen et al., 2011; Wasserburg et al., 2011). Significant neutron capture effects in Allende CAIs (including neutron capture on ^{35}Cl producing ^{36}Ar) were early reported by Göbel et al. (1982), but were attributed to GCR and not to SEP from the early Sun. Clear evidence of ^{36}Cl production by neutron capture was found in Allende fragments by Nishiizumi et al. (1986) by counting cosmic ray produced nuclei as a function of depth. In all cases the levels observed of neutron capture in Allende are far below that required to produce the value inferred from the Cl correlated ^{36}S excesses.

1.1. Production of ^{36}Ar and ^{38}Ar and deconvolution of their sources

There are four potential sources of the light isotopes of argon, ^{36}Ar and ^{38}Ar; (a) trapped argon (along with any possible adsorbed terrestrial atmosphere), characterised by $^{36}Ar/^{38}Ar = 5.25$. (b) cosmogenic argon from spallation reactions, principally on Ca, $^{36}Ar/^{38}Ar = 0.65$. (c) cosmogenic argon from the action of secondary neutrons on Cl, $^{36}Ar/^{38}Ar \sim 280$ (see below), and (d) ^{36}Ar from the decay of ^{36}Cl.

An unambiguous deconvolution of these four components requires four isotopes and is clearly not possible. Previous attempts to overcome this difficulty have been made by Jordan and Pernicka (1981) and by Göbel et al. (1982). The former, following a suggestion by Clayton (1977), made use of a comparison of ($^{38}Ar/^{36}Ar$) ratios as a function of release temperature from neutron irradiated and unirradiated aliquots of fine grained aggregates from Allende. The method they used made no distinction between contributions from spallogenic argon and trapped argon, treating them essentially as a single component of fixed composition. The ($^{38}Ar/^{36}Ar$) ratio of this component, which dominated the high temperature release, indicated a predominance of trapped argon in their samples of Allende. From the composition of a Cl-correlated component, tagged by neutron-induced ^{38}Ar in the irradiated aliquot, they inferred an upper limit of 1.2×10^{-8} for the ($^{36}Cl/^{35}Cl$) ratio.

Göbel et al. combined variations of $^{36}Ar/^{38}Ar$ as a function of temperature with upper and lower limits imposed by the ($^{38}Ar/^{36}Ar$) ratios of cosmogenic and trapped argon to estimate limits on the contribution from neutron capture in ^{35}Cl. From this they inferred a minimum value for $(^{36}Ar_{Cl}/^{35}Cl) = 7 \times 10^{-9}$ and a thermal neutron exposure of $\sim 1.5 \times 10^{14}$ cm^{-2}.

Neither method could distinguish ^{36}Ar from ^{36}Cl decay from ^{36}Ar produced together with small amounts of ^{38}Ar from the action of cosmogenic secondary neutrons on Cl. An alternative solution attempted here makes use of Ca to tag component (b), spallogenic argon. The effect of this is illustrated in Fig. 1. Unambiguous detection of ^{36}Ar from ^{36}Cl decay alone (as distinct from the decay of ^{36}Cl produced along with ^{38}Cl by cosmogenic secondary neutrons) would be indicated by data lying above the line joining the points labelled 'CR Spallation of Ca' and 'Secondary neutrons on Cl'. Ambiguities would still remain due to the possible presence of trapped Ar but, as we shall argue later, while trapped argon is present in Allende 'matrix', it appears to be absent in sodalite itself.

2. A SEARCH FOR CL-CORRELATED EXCESS ^{36}AR

2.1. Experimental method and results

In principle the $Ca/^{38}Ar$ ratio in Fig. 1 can be determined indirectly as $^{37}Ar/^{38}Ar$ using the familiar neutron irradiation techniques used in Ar–Ar dating. ^{37}Ar is generated by the reaction $^{40}Ca(n,\alpha)^{37}Ar$. However while neutron irradiation allows us to 'tag' the spallogenic component it introduces yet a fifth source of argon, namely ^{38}Ar from neutron

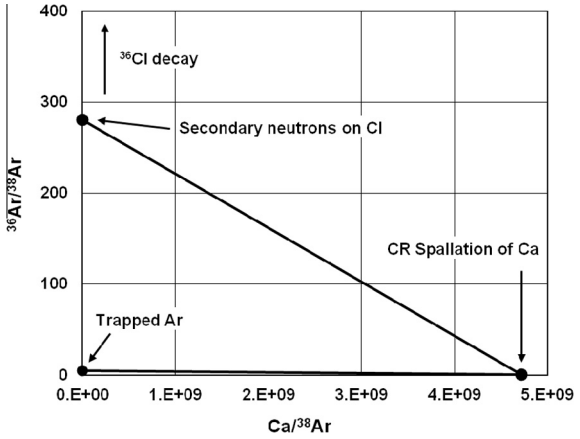

Fig. 1. Ar isotope mixing diagram to illustrate the principal of the present experiments, in which Ca is used to 'tag' the cosmogenic component.

absorption by ^{37}Cl, the reaction $^{37}Cl(n,\gamma,\beta^-)^{38}Ar$. Fortunately the contribution from this component, which lowers the Cl-correlated $^{36}Ar/^{38}Ar$ intercept, is a direct function of the irradiation fluence and as we demonstrate below can be eliminated by the use of two or more separate irradiations.

The neutron fluences typically used to date a typical 4.5 Gyr old meteorite by the ^{40}Ar–^{39}Ar method (Turner, 1971a), would produce overwhelming amounts of ^{38}Ar in the Cl-rich minerals sodalite and wadalite, and it is necessary to choose irradiation parameters which produce measurable ^{37}Ar from Ca while at the same time generating an amount of ^{38}Ar from Cl which is small or comparable to that from cosmogenic secondary neutrons. We have achieved this by the use of Cd shielding to minimise thermal neutron capture on ^{37}Cl, combined with the lowest practicable fast neutron fluence still capable of generating measurable ^{37}Ar from (n,α) reactions on ^{40}Ca.

We have analysed six neutron-irradiated samples from a friable 25 mg piece of Pink Angel taken from the sample described by Armstrong and Wasserburg (1981). Binocular inspection suggested that the six samples analysed contained abundant pink sodalite, and no attempt was made to generate representative aliquots. However determination of Cl/Ca ratios by neutron irradiation, as described below, showed some variability between 0.09 (molar) and 0.76, with a mean of 0.39 ± 0.26. Armstrong and Wasserburg (1981) list Cl/Ca ratios ranging from 1.09 for the interior of Pink Angel, in which the sodalite is concentrated, to 0.01 for the rim. The main carriers of Ca are diopside and anorthite, concentrated in the rim.

We irradiated six samples of Allende sodalite in the Cd-shielded CLICIT facility of the Oregon State TRIGA reactor. Two separate irradiations were performed; all six samples were included in the first. Following the analysis of three of these, a second irradiation was carried out on the remaining three. The time interval between the irradiations was such that, by the time of the second, ^{37}Ar from the first was completely decayed. A correction to add back this missing ^{37}Ar was applied, as described below.

Following the irradiations, argon isotopes from the two sets of sodalite-rich samples were extracted at increasing temperatures using a CW laser and analysed using the Noblesse mass spectrometer at the Open University. The results are given in the Electronic Annex (Tables A1 and A2). Because of the very low fluence used and the correspondingly very high $^{40}Ar/^{39}Ar$ ratios, the K–Ar information is unreliable, particularly for the first irradiation, and the tabulated data are restricted to ^{36}Ar, ^{37}Ar and ^{38}Ar. Hornblende Hb3gr was included in both irradiations to determine absolute conversion factors for the production of ^{38}Ar from Cl and ^{37}Ar from Ca. The fluence of irradiation 1 was too low to determine $(^{38}Ar/^{40}Ar)_{Hb}$ or $(^{37}Ar/^{40}Ar)_{Hb}$ owing to saturation of the ^{40}Ar signal. Fortunately these ratios were obtained for irradiation 2 and, together with $(^{38}Ar/^{37}Ar)_{Hb}$ for both irradiations (Table 1), can be used to determine the necessary conversion factors for the reactor irradiation and coincidentally a confirmation of the cosmic ray exposure age. The equations used to determine the conversion factors and the relationship to the exposure age are derived in the next section.

Table 1
Key argon isotope ratios.

	Irradiation 1	Irradiations 1 and 2
Measured		
$(^{36}Ar/^{38}Ar)_{intercept}$	139 ± 2	42.5 ± 1.0
$(^{37}Ar/^{38}Ar)_{cosmogenic}$	2.603 ± 0.035	9.2 ± 0.1
$(^{38}Ar^*/^{37}Ar^*)_{Hb3gr}$	$(8.57 \pm 0.60) \times 10^{-3}$	$(9.05 \pm 0.50) \times 10^{-3}$
$(^{37}Ar^*/^{40}Ar^*)_{Hb3gr}$	na	$(1.11 \pm 0.06) \times 10^{-3}$
Calculated		
$(P^{38}Ar.T_{exp})_{molar}$	$(2.12 \pm 0.05) \times 10^{-10}$	$(2.12 \pm 0.05) \times 10^{-10}$
$\langle\sigma_{40}.\Phi_R\rangle$	$(5.69 \pm 0.54) \times 10^{-10}$	$(2.01 \pm 0.05) \times 10^{-9}$
$\langle\sigma_{37}.\Phi_R\rangle/\langle\sigma_{40}.\Phi_R\rangle$	0.96 ± 0.06	1.01 ± 0.06

In Fig. 2 the results of the analyses are presented graphically, in a manner analogous to Fig. 1, as plots of $^{36}Ar/^{38}Ar$ against $^{37}Ar/^{38}Ar$. In the absence of trapped argon, the upper intercept of this plot is determined by the relative proportions of ^{36}Ar and ^{38}Ar from the action of cosmic ray-induced secondary neutrons, ^{36}Ar from the decay of ^{36}Cl, and ^{38}Ar from the reactor irradiation of Cl. The lower intercept (strictly at $^{36}Ar/^{38}Ar = 0.65$) is a function of the ratio of cosmogenic ^{38}Ar to Ca and the conversion factor of Ca to ^{37}Ar by the reactor irradiation.

The data from irradiation #1 for samples PA1 and PA2 lie on a well-defined mixing line (Fig. 2a) between a Ca-correlated cosmogenic end member with $^{37}Ar/^{38}Ar = 2.603 \pm 0.035$ ($^{36}Ar/^{38}Ar = 0.65$) and a Cl-correlated end member with $^{36}Ar/^{38}Ar = 139 \pm 3$ ($^{37}Ar/^{38}Ar = 0$). The absence of any significant deviations towards the composition of trapped argon at $^{36}Ar/^{38}Ar \sim 5.3$ and $^{37}Ar/^{38}Ar = 0$ suggests that the latter is absent. The data points show a systematic shift towards the Ca-correlated end member as the experiment progresses indicating greater retentivity of Ar in anorthite compared to sodalite. Sample PA3 is also consistent with the same mixing line but shows deviations towards the origin. These deviations may indicate the presence of trapped argon, possibly from presence in the sample of minor contamination by Allende matrix. An alternative explanation is that the contribution from ^{36}Cl decay is variable and absent in some areas of the sodalite.

The ^{38}Ar data for the irradiation #2 (Table A2 and Fig. 2b) includes a contribution from irradiation #1, whereas the ^{37}Ar produced in irradiation #1 had decayed prior to irradiation #2. To add back this decayed ^{37}Ar the measured ^{37}Ar has been multiplied by a factor of 1.59 ± 0.03. This factor was determined by adding lower intercept of Fig. 2a to the lower intercept of a similar plot of the uncorrected data from irradiation #2. The data from irradiation #2, including the lost ^{37}Ar from irradiation #1, (Fig. 2b) shows the anticipated linear trend for sample PA5, with upper and lower intercepts of 42.5 ± 1.0 and 9.2 ± 0.1. Sample PA4 trends towards the same lower intercept but, as with PA3, falls well below the line, either due to the presence of a 'matrix' component containing trapped argon, or due to the absence of ^{36}Ar from ^{36}Cl decay in this subsample. The data from sample PA6 are closer to those from PA5 but with small departures in the direction of the origin.

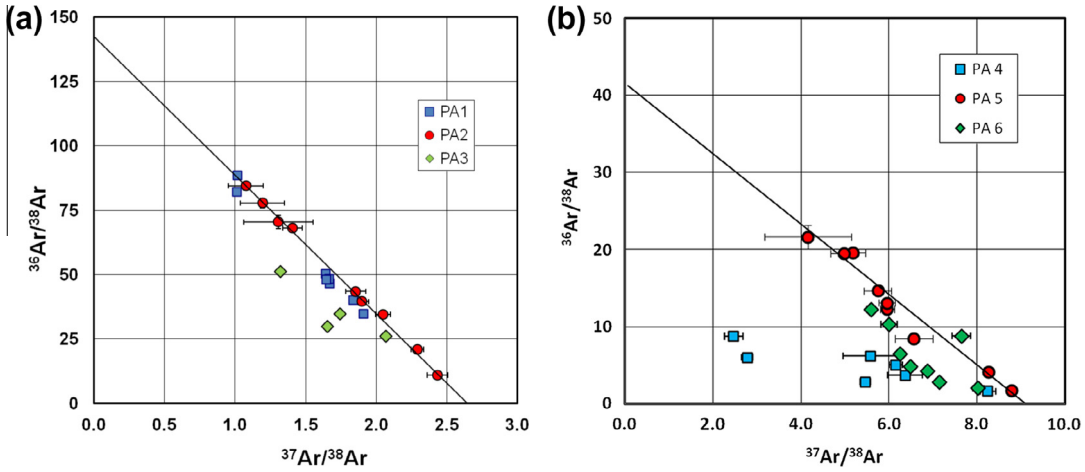

Fig. 2. Experimental data from two irradiations of Pink Angel sodalite using fluences differing by a factor of approximately 3.5.

2.2. Fluence monitoring

In principle the upper intercepts, $^{36}Ar/^{38}Ar$, of Fig. 2a and b contain contributions from three sources; ^{36}Ar from extinct ^{36}Cl decay, ^{36}Ar and ^{38}Ar from the action of cosmogenic secondary neutrons on Cl, and ^{38}Ar from the action of reactor neutrons on ^{37}Cl, i.e. $^{37}Cl(n,\gamma,\beta^-)^{38}Ar$. The lower intercept, $^{37}Ar/^{38}Ar$, contains ^{38}Ar from cosmic ray spallation of Ca and ^{37}Ar from the action of reactor neutrons on ^{40}Ca, i.e. $^{40}Ca(n,\alpha)^{37}Ar$.

In order to unscramble these components it is first necessary to quantify the reactor contributions by suitable fluence monitoring to determine absolute conversion factors for Cl and Ca. On account of the failure to measure ^{40}Ar in the neutron monitor Hb3gr in the first irradiation the derivations presented below are necessarily somewhat circuitous!

For both irradiations the $^{37}Ar/^{38}Ar$ ratio measured in the Hb3gr can be combined with the known Ca/Cl ratio of Hb3gr to determine the relative conversion factors.

We may write:

$$\langle\sigma_{40}.\Phi_R\rangle/\langle\sigma_{37}.\Phi_R\rangle = (^{37}Ar/^{38}Ar)_{Hb}.(^{37}Cl/^{40}Ca)_{Hb} \quad (1)$$

where the brackets represent the energy-averaged products of reactor neutron fluence, Φ_R and neutron absorption cross section, σ_{40} and σ_{37}, for ^{40}Ca and ^{37}Cl respectively. The subscript R is introduced to distinguish the reactor neutron fluence from the fluence of cosmic ray secondary neutrons, Φ_C (below).

As explained above we do not have absolute conversion factors for irradiation #1 due to saturation of the ^{40}Ar peak for Hb3gr. However for irradiation #2 the measured $^{37}Ar/^{40}Ar$ ratio in Hb3gr can be combined with the known ratio of ^{40}Ar to ^{40}Ca (Turner et al., 1971; Roddick, 1983) to determine the absolute conversion factor for ^{37}Ar from Ca, thus:

$$\langle\sigma_{40}.\Phi_R\rangle = (^{37}Ar/^{40}Ar)_{Hb3gr}.(^{40}Ar/^{40}Ca)_{Hb3gr} \quad (2)$$

Note that in using expression 2, the $(^{37}Ar/^{40}Ar)_{Hb3gr}$ ratio measured for irradiation #2 has been multiplied by the factor, 1.59 ± 0.03, referred to previously, to take account of the additional ^{37}Ar which would have been generated in the sample of Hb3gr used in irradiation #2 had it been included along with the sodalite in irradiation #1. The $(^{37}Ar/^{40}Ar)_{Hb3gr}$ ratio given in Table 1 is the value corrected for this decayed ^{37}Ar.

Independently of (2), $\langle\sigma_{40}.\Phi_R\rangle$ can be related to the cosmic ray exposure age of the sodalite and the $^{37}Ar/^{38}Ar$ ratio of the Ca-correlated end-member in Fig. 2 by the expression:

$$^{37}Ar_n/^{38}Ar_{sp} = (^{40}Ca/Ca).\langle\sigma_{40}.\Phi_R\rangle/(P_{38}.T_{exp}) \quad (3)$$

where subscripts n and sp refer to production by (reactor) neutrons and cosmic ray spallation respectively. P_{38} is the production rate of ^{38}Ar from spallation of Ca and T_{exp} the cosmic ray exposure age.

Substituting the values of $\langle\sigma_{40}.\Phi_R\rangle$ for Hb3gr and $^{37}Ar_n/^{38}Ar_{sp}$ for sodalite (from Fig. 2b) indicates a value of $P_{38}.T_{exp} = (2.12 \pm 0.05) \times 10^{-10}$ molar. This agrees within error with an estimate of $^{38}Ar_{sp}/Ca$ in Allende by Göbel et al. (1982) of $(10.8 \pm 2) \times 10^{-8}$ ccSTP/gCa, which corresponds to $P_{38}.T_{exp} = (1.93 \pm 0.36) \times 10^{-10}$.

The value of $\langle\sigma_{40}.\Phi_R\rangle$ for irradiation #1 has been calculated by substituting $(^{37}Ar_n/^{38}Ar_{sp})$ into expression (2) using our measured value of $P_{38}.T_{exp}$ above. By substituting the values for $\langle\sigma_{40}.\Phi_R\rangle$ into expression (1) we then calculate, for each irradiation, $\langle\sigma_{37}.\Phi_R\rangle$, the conversion factor from ^{37}Cl to ^{38}Ar. The measured parameters for Hb3gr and the corresponding conversion factors are summarised in Table 1.

2.3. ^{36}Cl and the Cl-correlated end member

Turning our attention to the upper intercepts of Fig. 2a and b, we may write:

$$^{36}Ar = {}^{35}Cl.\langle\sigma_{35}.\Phi_C\rangle.(1 - \tau_{36}/T_{exp}).B_{36} + {}^{35}Cl.(^{36}Cl/^{35}Cl)_o.B_{36} \quad (4)$$

and

$$^{38}Ar = {}^{37}Cl.[\langle\sigma_{37}.\Phi_C\rangle + \langle\sigma_{37}.\Phi_R\rangle] \quad (5)$$

Φ_C is the fluence of cosmogenic secondary neutrons, τ_{36} is the mean life of ^{36}Cl, and B_{36} the branching ratio for decay to ^{36}Ar (0.98). The factor $(1 - \tau_{36}/T_{exp})$ is the fraction of cosmogenic ^{36}Cl which has decayed to ^{36}Ar during T_{exp}, the cosmic ray exposure age (5 Ma in the case of Allende). This factor would be unity in cases where neutron exposure occurred in the distant past, for example in an ancient asteroidal regolith, as proposed by Bogard et al. (2001) to account for neutron induced ^{36}Ar in the Monahans halite. In the case of Allende, evidence linking ^{36}Ar excesses to ^{60}Co activity (Göbel et al., 1982) indicates that the neutron exposure responsible for generating ^{36}Ar and ^{38}Ar was recent.

Combining (1) and (2) and rearranging we obtain an expression relating the (unknown) primordial $(^{36}Cl/^{35}Cl)_o$ ratio to the (unknown) factor, $\langle\sigma_{35}.\Phi_C\rangle$, for production of ^{36}Ar from the irradiation of ^{37}Cl by cosmogenic secondary neutrons:

$$(^{36}Cl/^{35}Cl)_o = [(^{36}Ar/^{38}Ar).(^{37}Cl/^{35}Cl).\langle\sigma_{37}.\Phi_C\rangle/\langle\sigma_{35}.\Phi_C\rangle/B_{36} - (1-\tau_{36}/T_{exp})].\langle\sigma_{35}.\Phi_C\rangle + (^{36}Ar/^{38}Ar).(^{37}Cl/^{35}Cl).\langle\sigma_{37}.\Phi_R\rangle/B_{36} \quad (6)$$

To apply expression (6) the value of the ratio $\langle\sigma_{35}.\Phi_C\rangle/\langle\sigma_{37}.\Phi_C\rangle$ is also required. Fortunately $\langle\sigma_{35}.\Phi_C\rangle/\langle\sigma_{37}.\Phi_C\rangle$ is relatively independent of the neutron spectrum. For thermal neutrons the absorption cross sections are 43.6 ± 0.4 and 0.433 ± 0.006 barns, respectively. The corresponding resonance integrals for epithermal neutrons are 18 ± 2 and 0.295 ± 0.004 barns.

The only Cl-dominated sample for which estimates of $\langle\sigma_{35}.\Phi_C\rangle/\langle\sigma_{37}.\Phi_C\rangle$ have been published is halite from the Monahans chondrite. Wieler et al. (2000) measured $^{36}Ar/^{38}Ar = 204$ on an unirradiated sample, which corresponds to $\langle\sigma_{35}.\Phi_C\rangle/\langle\sigma_{37}.\Phi_C\rangle \sim 68$. Based on the very low $^{36}Ar/^{21}Ne$ ratio in the halite, Bogard et al. (2001) argue that it was irradiated at extremely shallow depth in an asteroidal regolith with a correspondingly hard secondary neutron spectrum. They suggest that $\langle\sigma_{35}.\Phi_C\rangle/\langle\sigma_{37}.\Phi_C\rangle \sim 77$ is appropriate. The large mass of Allende implies that in this case irradiation by thermal neutrons was more significant and in what follows we have used the ratio of the thermal neutron absorption cross sections, i.e. $\langle\sigma_{35}.\Phi_C\rangle/\langle\sigma_{37}.\Phi_C\rangle = 100$. However to test the effect of this assumption we have repeated our calculations with $\langle\sigma_{35}.\Phi_C\rangle/\langle\sigma_{37}.\Phi_C\rangle = 80$. As we shall show this has a negligible effect on our conclusions.

By substituting the measured values of $(^{36}Ar/^{38}Ar)$ and $\langle\sigma_{37}.\Phi_R\rangle$ for the two irradiations into expression (6) we obtain a pair of simultaneous equations which can be solved for $(^{36}Cl/^{35}Cl)_o$ and $\langle\sigma_{35}.\Phi_C\rangle$. The two equations are plotted in Fig. 3, their solution being determined by the point of intersection. The 1σ error limits are shown as dotted lines in the figure and have been calculated using a Monte Carlo method to propagate the uncertainties in the primary data. The intersection of the two lines indicates a non zero value for $(^{36}Cl/^{35}Cl)_o = (1.9 \pm 0.5) \times 10^{-8}$ and a cosmogenic secondary neutron fluence equivalent to $\langle\sigma_{35}.\Phi_C\rangle = (1.1 \pm 0.8) \times 10^{-8}$. Based on the thermal absorption cross section for ^{35}Cl this corresponds to a fluence of $(2.5 \pm 1.8) \times 10^{14}$ cm^{-2} s^{-1}.

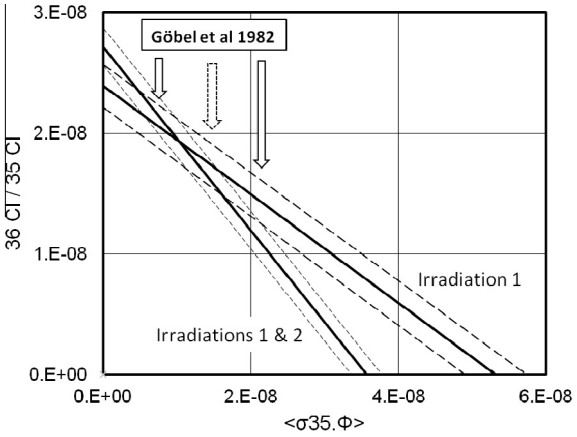

Fig. 3. Permitted combinations of $^{36}Cl/^{35}Cl$ and $\langle\sigma_{35}.\Phi_C\rangle$, the energy averaged product of cosmogenic secondary neutron fluence, Φ_C, and the ^{35}Cl neutron absorption cross section, σ_{35}, for the two irradiations. The actual values are given by the intersection of the two lines (solution to simultaneous Eq. (6)). As indicated, the value of $\langle\sigma_{35}.\Phi_C\rangle$ at the intersection is intermediate between the two extreme values for Allende measured by Göbel et al. (1982) and comparable to an estimate for Pink Angel based on ^{128}Xe production from ^{127}I (dashed arrow). Calculations assume $(\sigma_{35}/\sigma_{37}) = 100$.

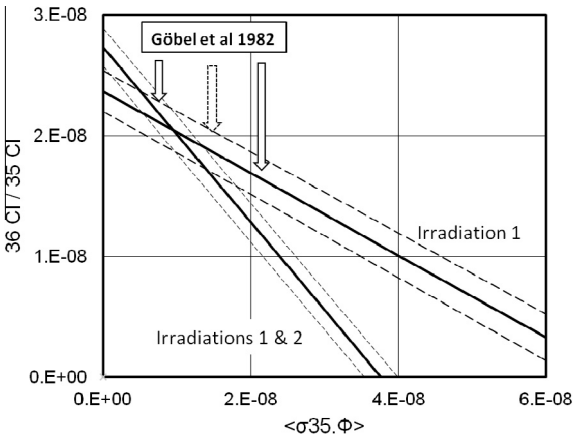

Fig. 4. As Fig. 3 but with the assumption that $(\sigma_{35}/\sigma_{37}) = 80$ (see text).

The effect of choosing $\langle\sigma_{35}.\Phi_C\rangle/\langle\sigma_{37}.\Phi_C\rangle = 80$ is illustrated in Fig. 4 and has a negligible effect on the solution to Eq. (6). The values for $(^{36}Cl/^{35}Cl)_o = (2.0 \pm 0.4) \times 10^{-8}$ and $\langle\sigma_{35}.\Phi_C\rangle = (1.0 \pm 0.6) \times 10^{-8}$ are indistinguishable from those based on thermal cross sections. The main effect is to lessen the slope of the line for irradiation 1 and make the horizontal intercept more extreme. Indeed it was the high value for this intercept (in Fig. 3), compared to the literature values, which led us to suspect the presence of excess ^{36}Ar from ^{36}Cl decay and perform the higher fluence irradiation.

Both figures illustrate the importance of the low fluence irradiation to provide a solution to Eq. (6). In the case of a high reactor fluence, for which $\langle\sigma_{37}.\Phi_R\rangle$ is significantly greater than $\langle\sigma_{37}.\Phi_C\rangle$, the figure degenerates into a single line with slope $-(1 - \tau_{36}/T_{exp})$. This can be readily

demonstrated by plotting the published data for high fluence irradiations of halite in the Monahans and Zag chondrites (Whitby et al., 2000; Bogard et al., 2001; Busfield et al., 2004).

Previous estimates of the product of fluence and cross section by Göbel et al. (1982) are shown in Fig. 3 and range from $\sim 0.5 \times 10^{-8}$ to 2.1×10^{-8} but as stated previously are unable to distinguish contributions to $^{36}Ar/^{35}Cl$ from extinct ^{36}Cl decay. The variation in the two estimates reflect real variation in secondary neutron flux within the Allende meteorite and are matched by a corresponding variation in the neutron induced $^{128}Xe/^{127}I$, from $\sim 4 \times 10^{-8}$ to 12×10^{-8} It is clear that cosmogenic neutron production can account for much if not all of their observed excess ^{36}Ar. The similarity with our estimate is evident.

Neutron induced $^{128}Xe/^{127}I$ can be used to make an independent estimate of $\langle \sigma_{35}.\Phi_C \rangle$ for the Pink Angel sodalite. The ratio $\langle \sigma_{35}.\Phi_C \rangle / \langle \sigma_{127}.\Phi_C \rangle$ is dependent on the extent to which the neutrons have been thermalised at depth in the meteoroid. Göbel et al. estimate values in the range 0.14–0.20 for Allende. Eberhardt et al. (1963) present an analytical model to estimate neutron spectra and production rates at depths within spheres of different radii. We have used this to calculate ratios from 0.15 at the surface to 0.3 at the centre of a 1 m radius chondritic object, which are comparable to the Göbel et al. measured values. For Pink Angel, Villa et al., (1981) estimate $^{128}Xe/^{127}I$, i.e. $\langle \sigma_{127}.\Phi_C \rangle$, equal to 8×10^{-8}. We have obtained a similar value, $\sim 7 \times 10^{-8}$, using RELAX (unpublished data). This is intermediate between the two Göbel et al. measurements, consistent with irradiation at an intermediate depth within Allende, and would correspond to an intermediate value of $\langle \sigma_{35}.\Phi_C \rangle \sim 1.4 \times 10^{-8}$. Our measured value is consistent with this independent estimate and significantly lower than the value of 5.3×10^{-8} which, as commented above, would be required to account for the data from irradiation #1 if $^{36}Cl/^{35}Cl$ were zero (lower intercept of Fig. 3).

Estimates of ($^{36}Cl/^{35}Cl$), based on excess ^{36}S, are variable and range from zero to 4×10^{-6} for Allende sodalite (Lin et al., 2005; Hsu et al., 2006; Ushikubo et al., 2007; Wasserburg et al., 2011), and 2×10^{-5} based on wadalite (Jacobsen et al., 2009, 2011), factors of up to 200 and 1000 respectively greater than the above value based on ^{36}Ar. Possible explanations of the low ^{36}Ar excess and the variability in ^{36}S involve details of how and under what conditions the ^{36}Cl was produced, the timing of sodalite deposition (Section 3), and the extent to which Ar was lost by thermal diffusion during or after deposition (Section 4).

3. I–XE CHRONOLOGY

The timing of sodalite formation is critical to constraining possible mechanisms responsible for the generation of short-lived ^{36}Cl. Evidence for an extended period of sodalite deposition several million years after formation of the solar system is provided by I–Xe dating. Xenon in meteoritic sodalite (and halite) is predominantly ^{129}Xe produced by the decay of now-extinct ^{129}I, reflecting the high iodine content associated with chlorine. Wasserburg and Huneke (1979) carried out I–Xe dating of Allende sodalite-rich inclusion 3509 and inferred a $^{129}I/^{127}I$ ratio $\sim 1.1 \times 10^{-4}$, indicating that the sodalite formed early in the history of the solar system. To determine a more precise chronology of sodalite formation, Swindle et al. (1988) carried out I–Xe studies of Pink Angel sodalite and Allende 'Egg' inclusions. An interior sample of Pink Angel yielded I–Xe ages ranging from 1.8 to 3.2 Ma after the chondrite Bjurbole, which they used as a monitor.

In the present study we have attempted to refine this chronology of sodalite formation further using the RELAX resonance ionisation mass spectrometer (Gilmour et al., 1994; Crowther et al., 2008) to perform I–Xe measurements on a core and two rim samples of the Pink Angel, and on the sodalite-rich inclusion, 3509, analysed by Wasserburg and Huneke (1979). Because of the very high sensitivity of RELAX and the rapid analysis time we have been able to carry out much higher resolution, i.e. many-step, analyses on samples of only a few tens of micrograms, in contrast to the milligram quantities analysed previously.

The samples were irradiated at the SAFARI-1 reactor in Pelindaba, South Africa with a thermal fluence, 7.5×10^{18} cm^{-2}, and fast fluence, 2.0×10^{18} cm^{-2}. Shallowater enstatite was included as an irradiation monitor. After irradiation, samples were loaded into the laser port of RELAX and analysed following the protocol described by Crowther et al. (2008). Gas was extracted from the samples by heating for one minute with a continuous wave Nd:YAG laser ($\lambda = 1064$ nm), at each of a series of sequentially increasing laser powers. Released gas was gettered for one minute to remove active gases, before being admitted into the mass spectrometer. Data were acquired in 30 consecutive ten-second segments. Isotope ratios and the height of a normalizing isotope calculated for the 30 segments were extrapolated to determine the corresponding quantities at the time of gas inlet. Absolute gas quantities were calculated and a discrimination correction made with reference to interspersed air calibrations. The procedural blank was monitored throughout the analyses but made negligible contribution to the isotopic data discussed here.

The results are presented graphically in Fig. 5 and in tabular form in Table A3 (Electronic Annex). $^{129}Xe/^{128}Xe$ ratios have been converted to absolute ages based on an assumed age of 4562.3 ± 0.4 Ma for the monitor Shallowater (Gilmour et al., 2009). The two rim samples trend upwards in age with temperature and are reproducible both in trend and in gas concentration. At intermediate temperatures the ages increase over a range of around a million years, approaching in the highest temperature extractions values close to that displayed by the interior sample W196P. The latter is more iodine-rich than the rim sample and yields ages which, within error, are identical for 61 extractions from 5% to 98% release. The age for Pink Angel alteration based on W196P is -2.89 ± 0.06 Ma relative to Shallowater (where the minus sign indicates more recent) corresponding to an absolute age for the alteration of 4559.4 ± 0.6 Ma.

Ages determined for sample 3509 are more scattered and older than W196P, by around 1.4 Ma in the intermediate release, rising to values close to Shallowater at higher temperatures. The ages obtained by Swindle et al. (1988) are

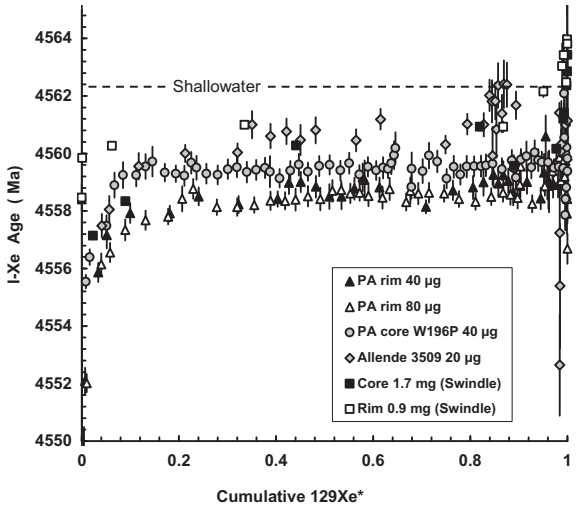

Fig. 5. I–Xe age spectra for Allende sodalites. The spread in ages indicates that the sodalite formed over an extended period of 2 Ma or so, around 4559 Ma ago, some 7 Ma after the formation of the host CAI. The higher ages in the very last extractions, especially those of Swindle et al. (1988), probably represent older Allende matrix or CAI.

also plotted in Fig. 5 and appear to be closer to 3509, both numerically and in the release pattern, than our analyses of the Pink Angel interior. However it is important to note that the Swindle et al. made use of the Bjurböle L4 chondrite as a monitor and at least some of the difference in the two sets of data may reflect actual variability in $^{129}Xe/^{127}I$ between individual Bjurböle chondrules (Gilmour et al., 2006). The use of Bjurböle as an I–Xe monitor has since been discontinued in favour of Shallowater. In the very highest temperature releases, the last one or two percent, both our data and those of Swindle et al. show a sharp rise in apparent age, of two or three million years. The most likely explanation of this is the contribution of minor amounts of xenon from an older, more retentive, iodine-poor CAI component unrelated to the sodalite.

The gradual increase in I–Xe ages with release step in the rim samples would conventionally be interpreted as reflecting diffusive loss of ^{129}Xe. However such an interpretation is difficult to reconcile with the exceptionally flat age pattern from the interior sample W196P and the spatial separation between rim and core of less than a centimetre. Diffusive loss from the rim alone would require flash heating with a duration less than the few seconds required for thermal diffusion to heat the interior. For this reason we are inclined to interpret the age pattern of the rim samples as reflecting an extended period of growth of the sodalite.

The main conclusions we draw from Fig. 5 are to confirm that the sodalite is significantly younger, by around seven million years, than the host CAI and that deposition occurred over an extended period of one or two million years.

4. DIFFUSION OF ARGON AND XENON

The presence in sodalite of ^{36}Ar a factor of 200 lower in abundance than that implied by the ^{36}S excesses, requires an explanation. Barber and Vaughan (1971) investigated the trapping of argon in the cage structure of synthetic sodalite and the subsequent diffusion kinetics as a function of temperature (see also Kopelevich and Chang, 2001). Expressing diffusion coefficient, D, as a function of temperature, T, in the familiar form:

$$D = D_o \exp(-E/RT) \quad (7)$$

They determined values for the activation energy, E, of 125 ± 2 kJ mol^{-1} K^{-1} and 112 ± 1 kJ mol^{-1} K^{-1}, for two synthetic samples prepared by different methods.

We have attempted to estimate values of E for ^{36}Ar diffusion in Allende sodalite based on the published data of Göbel et al. (1982) for their sample 3515, and to a lesser extent 3529, which showed large excesses of Cl-derived ^{36}Ar. The spreadsheet with calculations is included in the Electronic annex. Because of the very few data points this estimate is imprecise but suggests a value of E between 96 and 134 kJ mol^{-1} K^{-1}.

Our own data have more points but being the result of laser heating have no direct temperature estimates. We have sought to overcome this problem by combing the laser power measurements with the Stefan–Boltzmann law to estimate temperature. This required us to fix the temperature of one extraction, which we did by matching the Pink Angel (PA1) Arrhenius plot with that of the corresponding Göbel et al. plot at one temperature. The data and the plot are included in the Supplementary data and indicate an activation energy for the Cl-correlated ^{36}Ar and ^{38}Ar release of 126 kJ mol^{-1} K^{-1}. A similar calculation for the Ca-correlated, i.e. cosmogenic, ^{38}Ar indicates a higher activation energy of 166 kJ mol^{-1} K^{-1}, corresponding to diffusion from anorthite and to a lesser extent diopside.

In order to consider the possible extent of argon loss, during or after sodalite formation, we shall assume that the fractional loss is a function only of the integral $\int D.dt$ over time, t. We shall simplify this further by replacing the integral by D.t, where D and t are representative of a major loss episode. Using expression (7) we can then equate the fraction of argon loss in the past, during a period of heating at a temperature, T, for a time, t, to the *same loss* occurring in a laboratory heating experiment, at temperature T_o for time t_o, (Turner, 1971b, 1981; McConville et al., 1988):

$$1/T = 1/T_o + R/E \ln(t/t_o) \quad (8)$$

Expression (8) has been used to calculate the time-temperature combinations corresponding to 95% loss and 50% loss for activation energies of 110 kJ mol^{-1} K^{-1}and 130 kJ mol^{-1} K^{-1}. These are displayed in Fig. 6. The calculations, based on the data of Göbel et al., assume a laboratory heating time $t_o = 1800$ s, and that 50% loss occurs at 650 °C and 95% loss at 850 °C.

Notwithstanding the very long extrapolation (14 orders of magnitude in time) and the simple assumptions made regarding the scaling method, several general conclusions can be drawn:

(a) For time scales comparable to the half life of ^{36}Cl, substantial loss of ^{36}Ar from the sodalite could have arisen at elevated temperatures of 100–150 °C or so during its formation.

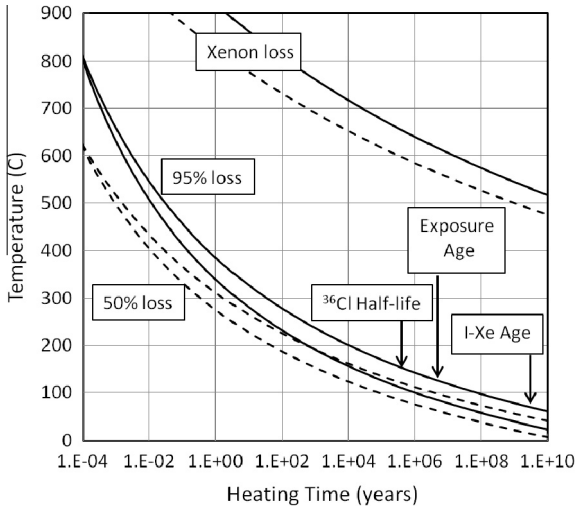

Fig. 6. Extrapolations of laboratory measurements of ^{36}Ar release from sodalite indicating the temperatures required for 50% and 95% loss over times up to the age of the solar system. The upper curve of each pair corresponds to an activation energy of 130 kJ^{-1} mol^{-1} K^{-1}, the lower to 110 kJ^{-1} mol^{-1} K^{-1}. The curves indicate the ease with which Ar may diffuse out of sodalite over geological times. The curves labelled Xenon loss are for 50% and 95% xenon release based on an activation energy of 450 kJ^{-1} mol^{-1} K^{-1}inferred from the data of Swindle et al. (1988).

(b) The retention of ^{36}Ar and ^{38}Ar produced by cosmogenic secondary neutrons implies that temperatures did not exceed 0 °C significantly during the last 5 Ma.
(c) It is likely that significant loss of ^{36}Ar generated by ^{36}Cl decay could have occurred during the last 4.5 Ga, although to lose 99.9% probably implies elevated temperatures, early in the history of the sodalite.

The diffusion properties of xenon in Pink Angel are at least as significant to understanding the origin of ^{36}Cl as those of argon. Mechanisms proposed to account for the generation of ^{36}Cl involve high fluences of thermal or epithermal neutron during a t-tauri phase of the early sun. In addition to ^{36}Cl this would generate substantial amounts of ^{128}Xe from the high concentrations of iodine associated with chlorine-rich fluids. Xenon is likely to be retained in solid phases more effectively than argon and in order to quantify this we have attempted to make estimates of activation energy and release temperatures for xenon in sodalite using the published data of Swindle et al. (1988). Our analysis of their data is included in the Supplementary data tables and leads to an estimate of around 450 kJ mol^{-1} K^{-1} for the activation energy, a temperature of around 1100 °C for 50% release and 1250 °C for 95% release. These estimates have been applied to expression (8) and plotted alongside the curves for argon loss in Fig. 6. Despite the uncertainties in the extraction temperatures quoted by Swindle et al., it is difficult to avoid the conclusion that loss of xenon from sodalite requires very high temperatures, $\geqslant$600 °C, even for loss over geological time scales.

5. SUMMARY AND DISCUSSION

In summary we have:

(a) Devised a method to distinguish ^{36}Ar from the decay of ^{36}Cl in the presence of ^{36}Ar and ^{38}Ar from the action of secondary cosmic ray neutrons on chlorine.
(b) Applied this method to sodalite in the Allende meteorite and demonstrated the presence of small amounts of ^{36}Ar from the decay of now-extinct ^{36}Cl.
(c) Inferred a ^{36}Cl/^{35}Cl ratio of $(1.9 \pm 0.5) \times 10^{-8}$ which is a factor of 200 lower than the highest value inferred from published ^{36}S excesses in sodalite.
(d) Determined the cosmogenic secondary neutron exposure of the sodalite as the energy averaged product of fluence and neutron absorption cross section, $\langle \sigma_{35}.\Phi_C \rangle = (1.1 \pm 0.8) \times 10^{-8}$. Based on the thermal absorption cross section for ^{35}Cl this corresponds to a fluence of $(2.5 \pm 1.8) \times 10^{14}$ cm^{-2} s^{-1}.
(e) Confirmed and extended the chronology of the sodalite formation using high resolution I–Xe measurements which confirm that the sodalite is significantly younger, by around seven million years, than the host CAI and that deposition occurred over an extended period of one or two million years.
(f) For one particular specimen, W196P, obtained a precise I–Xe age, based on a 61 point isochron, of 4559.4 ± 0.6 Ma.
(g) Based on the release pattern of ^{36}Ar as a function of temperature, inferred an activation energy for Ar diffusion in Allende sodalite of ~126 kJ mol^{-1} K^{-1}. This is comparable to published measurements based on trapping and diffusion in synthetic sodalite.
(h) Based on this low activation energy for Ar diffusion, deduced that loss of ^{36}Ar by thermal diffusion may have occurred, either during the time of sodalite formation or over the succeeding 4.5 Ga.
(i) Based on published data, calculated that loss of xenon over geological time scales by thermal diffusion requires substantially elevated temperatures, $\geqslant$600 °C and conclude that its absence in Pink Angel sodalite places a severe constraint on models for the production of ^{36}Cl.

The ability to distinguish ^{36}Ar produced by ^{36}Cl decay from that produced by the action of secondary neutrons on Cl appears to have solved a long-standing puzzle. The critical feature of our measurements is the observation of the high intercept, ^{36}Ar/^{38}Ar $= 139 \pm 3$, in Fig. 2(a), which leads in turn to an estimate for the product of the cosmogenic secondary neutron fluence and cross section, $\langle \sigma_{35}.\Phi_C \rangle = 5.2 \times 10^{-8}$, *if it is assumed that there is no contribution from ^{36}Cl decay*. As stated previously, this unexpectedly high value for $\langle \sigma_{35}.\Phi_C \rangle$, compared to published values for other samples of Allende, led us to perform the second higher fluence irradiation, leading to the identification of a contribution from ^{36}Cl decay, exemplified by Fig. 3.

We now consider the implications of low levels of ^{36}Ar from ^{36}Cl decay in the sodalite. In view of the ease with

which Ar may be lost by thermal diffusion it is evident that the ^{36}Ar we observe must have been generated in-situ in the sodalite. On the assumption that the ^{36}Cl was formed by intense neutron irradiation (Hsu et al., 2006; Jacobsen et al., 2011; Wasserburg et al., 2011) such as might have resulted from a t-tauri stage of solar evolution several key questions arise: What was the duration of the neutron exposure? Was the ^{36}Cl formed in-situ in the sodalite or in a pre-existing Cl-rich environment, such as the metasomatising fluid responsible for depositing the sodalite (Wasserburg et al., 2011). To what extent does the low ^{36}Cl/^{35}Cl ratio inferred from ^{36}Ar have chronological implications, indicating the time at which retention of ^{36}Ar from ^{36}Cl decay began (closure against diffusive loss) or to what extent is it the result of subsequent diffusive loss.

The absence of large amounts of neutron generated ^{128}Xe in the sodalite, beyond that resulting from cosmogenic secondary neutrons, is critical to the question whether or not the ^{36}Cl could have been generated directly in the sodalite by neutron irradiation. The low level of ^{128}Xe, would require almost total diffusive loss of Xe, during and after the irradiation, until lowering of the temperature permitted first radiogenic ^{129}Xe, and later ^{36}Ar, to be retained during the final stages of ^{36}Cl decay. The necessary conditions, reflected in the plots for argon and xenon retention in Fig. 6, place constraints on the possible time-temperature histories. Loss of most of the ^{128}Xe, over time scales of a few million years, would imply temperatures in excess of 600 °C during the irradiation, falling, in a million years or less, to below 100 °C to permit retention of ^{36}Ar. These constraints argue against generation of the ^{36}Cl directly in the sodalite.

A more likely scenario, that ^{36}Cl was produced by neutron irradiation of a Cl-rich fluid (Wasserburg et al., 2011), the precursor of the sodalite, is less restrictive. It has no difficulty in accounting for the apparent absence of ^{38}Ar and ^{128}Xe, which, along with ^{36}Ar, would escape from the fluid. However it leads to a range of options to account for the Cl-correlated ^{36}S anomaly, depending on the extent to which the sodalite deposition occurred before substantial ^{36}Cl decay had occurred, or later with some of the ^{36}S excess introduced as a 'fossil' decay product.

We may write down a simple expression describing the problem. For a uniform irradiation of duration T, the total amount of ^{36}Cl generated is P.T, where P is the production rate. Note that P is likely to show some variation as a result of spatial variability in the neutron fluence within the solar nebula and between different fluid sites. For a particular value of P, the build up of ^{36}Cl is given by the familiar expression $(P.\tau).(1 - \exp(-T/\tau))$, reaching a secular equilibrium value $P.\tau$ after a few half lives of ^{36}Cl. If the sodalite formed a time, t_s, after the end of the neutron irradiation, the level of ^{36}Cl at this time would be $(P.\tau).(1 - \exp(-T/\tau)).\exp(-t_s/\tau)$. We assume that build up and retention of excess ^{36}S began at this time and corresponds to the I–Xe age. Furthermore, if ^{36}Ar retention in the sodalite began a time, t_c (closure time), after the end of the neutron irradiation, the level of ^{36}Cl at this later time would be $(P.\tau).(1 - \exp(-T/\tau)).\exp(-t_c/\tau)$. Depending on the extent of subsequent diffusive loss of ^{36}Ar, the value of ^{36}Cl/^{35}Cl inferred from ^{36}Ar will differ from that inferred from ^{36}S, by a factor less than or equal to $\exp(-(t_c - t_s)/\tau)$. Substituting $\exp(-(t_c - t_s)/\tau) \geqslant 1/200$, indicates $(t_c - t_s) \leqslant 2.3$ Ma.

This calculation has no implications concerning the duration of the neutron irradiation, T, other than $(T + t_s)$ must be less than the 7 Ma time interval between the formation of CAI and the closure of sodalite to Xe loss indicated by the I–Xe age. The effect of T is to determine the proportion of ^{36}Cl which survives at the end of the irradiation, prior to incorporation in sodalite. This is $(\tau/T).(1 - \exp(-T/\tau))$, which approaches unity for a short irradiation with $T \leqslant \tau$. For long duration irradiations, i.e. $T \gg \tau$, the proportion of ^{36}Cl surviving is small, τ/T, leading to a corresponding build up of excess ^{36}S in the fluid. The fate of this ^{36}S, in particular the extent to which it remains in the fluid or is lost, has a bearing on the interpretation of the ^{36}S excesses in sodalite.

The observed correlations between δ^{36}S and Cl/S in sodalite are generally taken to be evidence for in-situ decay of ^{36}Cl. However in the case of an irradiation of a few million years it is conceivable that excess ^{36}S from ^{36}Cl decay could be retained in the precursor fluid and introduced subsequently into the sodalite as a monoisotopic 'spike'. In this case the correlation between δ^{36}S and Cl/S could, in principle, represent a mixing line between Cl-correlated excess ^{36}S and variable low levels of normal sulphur. To maintain a well defined pseudo-isochron would require that the trace amounts of excess ^{36}S be incorporated along with its 'parent' Cl without significant fractionation. During an irradiation of several million years ^{36}Cl/^{35}Cl would reach secular equilibrium, at a level roughly one tenth of that inferred from the slope of the δ^{36}S and Cl/S mixing line, i.e. $\sim 4 \times 10^{-7}$. In this case the value of 2×10^{-8} deduced from the ^{36}Ar excess would correspond to ^{36}Cl decay over an interval of 1.3 Ma between deposition of the sodalite and onset of ^{36}Ar retention. Subsequent diffusive loss would reduce this estimate by 0.3 Ma for each factor 2 depletion of ^{36}Ar.

In this report we have presented unambiguous evidence for ^{36}Ar produced by the decay of now extinct ^{36}Cl in the first few million years of solar system history. We have also proposed mechanisms which can account for the disparity between the ^{36}S excesses and the much smaller ^{36}Ar excess. The preferred mechanisms involve neutron irradiation of a Cl-rich fluid during a t-tauri phase of the sun, subsequent deposition of sodalite, ^{36}Cl decay before and after sodalite deposition, loss of neutron generated ^{128}Xe and partial loss of ^{36}Ar from ^{36}Cl decay. These explanations are not unique but importantly make different predictions as to the presence or absence of ^{36}S anomalies, and of ^{128}Xe and ^{36}Ar excesses at different times. Seeking these anomalies in a range of samples in combination with precise high resolution I–Xe ages could provide clarification.

ACKNOWLEDGEMENTS

We thank J. Cowpe, D. Blagburn and B. Clementson for technical support. The work was funded by the Science and Technology Facilities Council through grants ST/J001643/1 and ST/G003068/1. G.J.W acknowledges support by a NASA Cosmochemistry RTOP to J. Nuth, at GSFC, and by the Epsilon Foundation.

APPENDIX A. SUPPLEMENTARY DATA

Supplementary data associated with this article can be found, in the online version, at http://dx.doi.org/10.1016/j.gca.2013.06.022.

REFERENCES

Armstrong J.T. and Wasserburg G. J. (1981) The allende pink angel: its mineralogy, petrology, and the constraints of its genesis. *Lunar Planet. Sci. XII*. Lunar Planet. Inst., Houston. 25–27.

Barber R. M. and Vaughan D. E. W. (1971) Trapping of inert gases in sodalite and cancrite crystals. *J. Phys. Chem. Solids* **32**, 731–743.

Bogard D. D., Garrison D. H. and Masarik J. (2001) The Monahans chondrite and halite: Argon-39/argon-40 age, solar gases, cosmic-ray exposure ages, and parent body regolith neutron flux and thickness. *Meteorit. Planet. Sci.* **36**, 107–122.

Busfield A., Gilmour J. D., Whitby J. A. and Turner G. (2004) Iodine–xenon analysis of ordinary chondrite halide: Implications for early solar system water. *Geochim. Cosmochim. Acta* **68**, 195–202.

Clayton D. D. (1977) Interstellar potassium and argon. *Earth Planet. Sci. Lett.* **36**, 381–390.

Crowther S. A., Mohapatra R. K., Turner G., Blagburn D. J., Kehm K. and Gilmour J. D. (2008) Characteristics and applications of RELAX, an ultrasensitive resonance ionization mass spectrometer for xenon. *J. Anal. At. Spectrom.* **23**, 938–947.

Eberhardt P., Geiss J. and Lutz H. (1963) Neutrons in meteorites. In Earth Science and Meteoritics (Ed. J. Geiss and E. D. Goldberg), p. 143 - 168, North Holland Publ. Comp., Amsterdam.

Gilmour J. D., Lyon I. C., Johnston W. A. and Turner G. (1994) RELAX: An ultrasensitive resonance ionization mass spectrometer for xenon. *Rev. Sci. Instrum.* **65**, 617–625.

Gilmour J. D., Pravdivtseva O. V., Busfield A. and Hohenberg C. M. (2006) The I–Xe chronometer and the early solar system. *Meteorit. Planet. Sci.* **41**, 19–31.

Gilmour J. D., Crowther S. A., Busfield A., Holland G. and Whitby J. A. (2009) An early I–Xe age for CB chondrule formation, and a re-evaluation of the closure age of Shallowater enstatite. *Meteorit. Planet. Sci.* **44**, 573–579.

Göbel R., Begemann F. and Ott U. (1982) On neutron-induced and other noble gases in Allende inclusions. *Geochim. Cosmochim. Acta* **46**, 1777–1792.

Hsu W., Guan Y., Leshin L. A., Ushikubo T. and Wasserburg G. J. (2006) A late episode of irradiation in the early solar system: Evidence from extinct ^{36}Cl and ^{26}Al in meteorites. *Astrophys. J.* **640**, 525–529.

Jacobsen B., Matzel J., Hutcheon I. D., Ramon E., Krot A. N., Ishii H. A., Nagashima K. and Yin Q. Z. (2009) The 36Cl-36S systematics of wadelite from the Allende meteorite. *Lunar Planet. Sci. XL*. Lunar Planet. Inst., Houston. 2553–2554.

Jacobsen B., Matzel J., Hutcheon I. D., Krot A. N., Yin Q. Z., Nagashima K., Ramon E. C., Weber P. K., Ishii H. A. and Ciesla (2011) Formation of the short-lived radionuclide ^{36}Cl in the protoplanetary disk during late-stage irradiation of a volatile-rich reservoir. *Astrophys. J. Lett.* **731**, L28 (6pp).

Jordan J. and Pernicka E. (1981) Search for extinct ^{36}Cl in Allende. *Meteoritics* **16**, 332–333.

Kopelevich D. I. and Chang H. C. (2001) Diffusion of inert gases in silica sodalite: Importance of lattice flexibility. *J. Chem. Phys.* **115**, 9519–9527.

Lin Y., Guan Y., Leshin L. A., Ouyang Z. and Wang D. (2005) Short-lived chlorine-36 in a Ca- and Al-rich inclusion from the Ningqiang carbonaceous chondrite. *Proc. Natl. Acad. Sci. U.S.A.* **102**, 1306–1311.

McConville P., Kelley S. and Turner G. (1988) Laser probe ^{40}Ar–^{39}Ar studies of the Peace River shocked L6 chondrite. *Geochim. Cosmochim. Acta* **52**, 2487–2499.

Nishiizumi K., Elmore D., Kubik P. W., Bonani G., Suter M., Wolfli W. and Arnold J. R. (1986) Age of Antarctic meteorites and ice II. *Lunar Planet. Sci.* **17**, 18–20.

Roddick J. C. (1983) High precision intercalibration of ^{40}Ar–^{39}Ar standards. *Geochim. Cosmochim. Acta* **47**, 887–898.

Swindle T. D., Caffee M. W. and Hohenberg C. M. (1988) Iodine–xenon studies of Allende inclusions: Eggs and the Pink Angel. *Geochim. Cosmochim. Acta* **52**, 2215–2227.

Turner G. (1971a) Argon 40–argon 39 dating: The optimization of irradiation parameters. *Earth Planet. Sci. Lett.* **10**, 227–234.

Turner G. (1971b) ^{40}Ar–^{39}Ar ages from the Lunar maria. *Earth Planet. Sci. Lett.* **11**, 169–191.

Turner G. (1981) Argon–argon age measurements and calculations of temperatures resulting from asteroidal break-up. *Proc. R. Soc. London* **A374**, 281–298.

Turner G., Huneke J. C., Podosek F. A. and Wasserburg J. G. (1971) ^{40}Ar–^{39}Ar ages and cosmic ray exposure ages of Apollo 14 samples. *Earth Planet. Sci. Lett.* **12**, 19–35.

Ushikubo T., Guan Y., Hiyagon H., Sugiura N. and Leshin L. A. (2007) ^{36}Cl, ^{26}Al and O isotopes in an Allende type B2 CAI: Implications for multiple secondary events in the early solar system. *Meteorit. Planet. Sci.* **42**, 1267–1279.

Villa I. M., Huneke J. C., Papanastassiou D. A. and Wasserburg G. J. (1981) The allende pink angel: chronological constraints from Xe, Ar, and Mg. *Lunar Planet. Sci. XII*. Lunar Planet. Inst., Houston. 1115–1117 (abstr.).

Wasserburg G. J. and Huneke J. C. (1979) I–Xe dating of I-bearing phases in Allende. *Lunar Planet. Sci.* **X**, 1307–1309.

Wasserburg G. J., Hutcheon I. D., Aléon J., Ramon E. C., Krot A. N., Nagashima K. and Brearley A. J. (2011) Extremely Na- and Cl-rich chondrule from the CV3 carbonaceous chondrite Allende. *Geochim. Cosmochim. Acta* **75**, 4752–4770.

Whitby J., Burgess R., Turner G., Gilmour J. and Bridges J. (2000) Extinct ^{129}I in halite from a primitive meteorite: Evidence for an evaporate formation in the early solar system. *Science* **288**, 1819–1821.

Wieler R., Günther D., Hattendorf B., Leya I., Pettke T., Vogel N. and Zolensky M. E. (2000) The chemical composition and light noble gas data of halite in the Monahans regolithic breccia. *Meteorit. Planet. Sci.* **35**, A170.

Associate editor: Anders Meibom